Hindawi Publishing Corporation
Advances in Materials Science and Engineering
Volume 2014, Article ID 245473, 13 pages
http://dx.doi.org/10.1155/2014/245473

*Research Article*

# The Effect of Variation of Molarity of Alkali Activator and Fine Aggregate Content on the Compressive Strength of the Fly Ash: Palm Oil Fuel Ash Based Geopolymer Mortar

**Iftekhair Ibnul Bashar, U. Johnson Alengaram, Mohd Zamin Jumaat, and Azizul Islam**

*Department of Civil Engineering, Faculty of Engineering, University of Malaya, 50603 Kuala Lumpur, Malaysia*

Correspondence should be addressed to U. Johnson Alengaram; ujohnrose@yahoo.com

Received 24 February 2014; Revised 11 June 2014; Accepted 13 June 2014; Published 20 July 2014

Academic Editor: Dachamir Hotza

Copyright © 2014 Iftekhair Ibnul Bashar et al. This is an open access article distributed under the Creative Commons Attribution License, which permits unrestricted use, distribution, and reproduction in any medium, provided the original work is properly cited.

The effect of molarity of alkali activator, manufactured sand (M-sand), and quarry dust (QD) on the compressive strength of palm oil fuel ash (POFA) and fly ash (FA) based geopolymer mortar was investigated and reported. The variable investigated includes the quantities of replacement levels of M-sand, QD, and conventional mining sand (N-sand) in two concentrated alkaline solutions; the contents of alkaline solution, water, POFA/FA ratio, and curing condition remained constant. The results show that an average of 76% of the 28-day compressive strength was found at the age of 3 days. The rate of strength development from 3 to 7 days was found between 12 and 16% and it was found much less beyond this period. The addition of 100% M-sand and QD shows insignificant strength reduction compared to mixtures with 100% N-sand. The particle angularity and texture of fine aggregates played a significant role in the strength development due to the filling and packing ability. The rough texture and surface of QD enables stronger bond between the paste and the fine aggregate. The concentration of alkaline solution increased the reaction rate and thus enhanced the development of early age strength. The use of M-sand and QD in the development of geopolymer concrete is recommended as the strength variation between these waste materials and conventional sand is not high.

## 1. Introduction

The depletion of natural resources leads to ecological imbalance globally and its effect has been felt in civil engineering more than any other field of engineering. In order to ensure sustainable development, researchers all around the world have focused their research on replacing and recycling waste materials to replace conventional materials [1–4]. Millions of tons of industrial wastes are generated every year and these wastes cause environmental issue due to shortage of storage facility; this subsequently leads to land and water pollution in the vicinity of factories.

The quarry industries produce millions of tons of wastes in the form of quarry dust (QD); it is produced as waste after crushing granite for the use of coarse aggregates. About 25% QD is produced from the coarse aggregate production by stone crusher [5]. These wastes are dumped in the factory yards and hence reuse of QD might help in reducing the overuse of mining and quarrying. The sophisticated technology known as vertical shaft impact (VSI) crusher system allows QD to be centrifuged to remove flaky and sharp edges. The end product is commonly known as manufactured sand (M-Sand) and it is popular in some of the developing countries [6]; the use of M-sand and QD is in the right direction to achieve sustainable material.

The main characteristics of the fine aggregate that affect the compressive strength of fresh and hardened concrete are shape, grade, and maximum size. The factors such as shape and texture of the fine aggregate affect the workability of fresh concrete and also influence the strength and durability characteristics of hardened concrete. The spherical particles have less surface area than the particles with flat surface and elongated shape. The cubical and spherical shape contributes to good workability with less water [7]. Flaky and elongated particles have negative effect on workability, producing very harsh mixtures. For given water content, these poorly shaped

particles lead to less workable mixtures than cubical or spherical particles. Conversely, for given workability, flaky and elongated particles increase the demand for water thus affecting strength of hardened concrete. The void content is also affected by angularity.

In fact, the angular particles tend to increase the demand for water as these particles increase the void content compared to rounded particles [8]. The rough aggregate increase the water demand for given workability [9]. Since N-sand is often rounded and smooth compared to M-sand, N-sand usually requires less water than M-sand for given workability [8]. However, workable concrete can be made with angular and rough particles if they are cubical and well graded.

Besides the depletion of natural resources, another environmental problem is the greenhouse effect. One of the main reasons for the greenhouse effect is the emission of carbon dioxide ($CO_2$) from the ordinary Portland cement (OPC) based concrete production. Marceau et al. [10] stated that about 60% of $CO_2$ emission was due to the OPC production. The development of cement less concrete is a big challenge to the researchers nowadays. Davidovits [11] is the pioneer in introducing geopolymer concrete which emits no $CO_2$. Thokchom et al. [12] investigated the performance of geopolymer mortar and found excellent performance in terms of durability with less weight loss. Silica and alumina are the main compounds to activate the geopolymerization process. The raw materials consisting of silica and alumina are known as pozzolanic material. Rukzon and Chindaprasirt [2] studied the resistance of sulphate attack of cement for different proportion of replacement by palm oil fuel ash (POFA), fly ash (FA), and rice husk ash (RHA) and reported that POFA, FA, and RHA have a potentiality to be pozzolanic material. POFA and FA are two readily available industrial by-products; those could be the right choice as pozzolanic materials in the development of geopolymer concrete [13, 14]. Žvironaitė et al. [15] studied the effect of different pozzolans on the hardening process of binder.

The use of industrial by-product such as FA, silica fume (SF), ground granulated blast furnace slag (GGBS), metakaolin, bottom ash, and quarry fines, in the development of sustainable materials has substantially reduced pollution [16–20]. In southeast Asian countries such as Malaysia, Thailand, and Indonesia, the abundance of waste materials such as RHA, POFA, FA, GGBS, oil palm shell (OPS), and palm oil clickers has given right platform for researchers to explore the possibility of converting these wastes into potential construction materials [21–26].

About 85% of world's palm oil is being produced in Indonesia and Malaysia [27]. Therefore, the development of green concrete using these two industrial by-products, namely, POFA and FA, could enhance the use of the local waste material to develop sustainable concrete. The use of POFA in concrete industry as a cementing material reduces the environmental and health problems [4]. Altwair et al. [23] stated that concrete containing POFA improved the flexure deflection capacity and reduced the crack width. Altwair et al. [28] also reported that POFA had a good influence in achieving strain-hardening behavior and it enhanced the fracture toughness. Safiuddin et al. [21] improved the segregation resistance self-consolidated concrete incorporating POFA. Lim et al. [22] reported that foamed concrete incorporating POFA enhanced compressive, flexure, splitting tensile strength, and ductility. Hawa et al. [29] evaluated the performance and microstructure characterization of metakaolin based geopolymer concrete containing POFA.

Wallah and Rangan [30] and Hardjito et al. [31] introduced fly ash (FA) in geopolymer concrete as a complete replacement of cement. Further the benefit of using industrial by-products such as fly ash, palm oil shells also known as oil palm shells (OPS) in the development of lightweight concrete has been detailed by Chandra and Berntsson [16]. The engineering properties of high-strength lightweight OPS concrete with the replacement of cement by different proportion of FA were investigated [17]. Johnson Alengaram et al. [19] compared the thermal conductivity between OPS foamed concrete and conventional concrete. Kupaei et al. [32] proposed an appropriate mix design for geopolymer concrete using the two waste materials OPS and FA.

Since the geopolymer concrete/mortar utilizes waste materials such as POFA, FA, M-sand, QD, OPS, and other industrial wastes, the researches on geopolymer lead to sustainable material. The purpose of this paper therefore is to investigate the effect of M-sand and QD in POFA-FA-based geopolymer mortar in developing compressive strength.

## 2. Materials and Methods

*2.1. Material Collection and Preparation.* The POFA and FA were collected locally from Jugra Palm Oil Mill and Lafarge Malayan Cements, respectively. The M-sand and QD were supplied by Batu Tiga Quarry Sdn Bhd, a subsidiary of YTL Cements.

The raw POFA was sieved through 300 $\mu$m size sieve and then dried in an oven before being ground 30,000 cycles in 16 hours in a grinding machine. Forty mild steel rods of 10 mm diameter and 400 mm length were placed in the Los Angeles grinding machine to grind the POFA. FA was stored in air tight containers. The fine aggregate (N-sand, M-sand, and QD) were dried, sieved through 5 mm sieve, and retained on 300 $\mu$m sieve then were used in the preparation of geopolymer mortar.

*2.2. Chemical Composition and Particle Size Distribution of POFA and FA.* Figure 1 shows the powder forms of POFA and FA. The POFA and FA particles sieved through 45 $\mu$m have been used for both XRF and the particle size distribution tests. The chemical compounds of POFA and FA were determined using PANalytical X-ray fluorescence (XRF) machine through Omnian analysis. The particle size distribution was done by particle size analyzer through polydisperse analysis. The test results on X-ray fluorescence (XRF) for chemical composition and particle size distribution of POFA and FA are shown in Figure 2 and Table 1.

The percentages of $SiO_2$, $Al_2O_3$, and $Fe_2O_3$ are 76.14 and 87.15 in POFA and FA, respectively. According to ASTM C618, the POFA and FA are categorized as class F, since these samples contain at least 70% of $SiO_2$, $Al_2O_3$, and $Fe_2O_3$.

(a) (b)

Figure 1: (a) Palm oil fuel ash (POFA) and (b) Fly ash (FA).

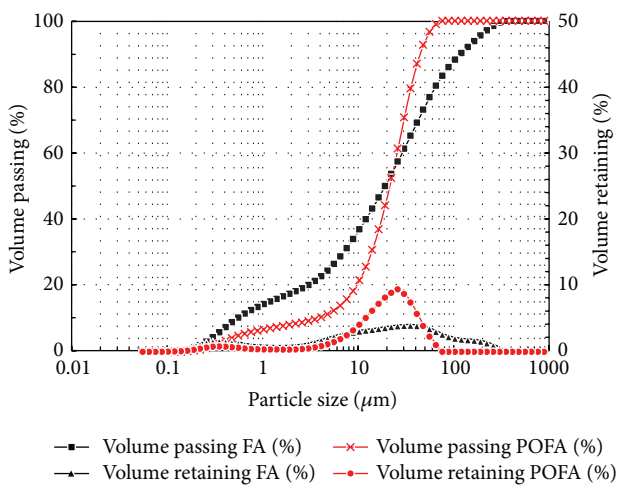


Figure 2: Particle size distribution of POFA and FA.

The ratio of POFA to FA used in this investigation was 1 : 1; therefore, $SiO_2 : Al_2O_3$ in POFA and FA was 3.95 : 1.

*2.3. Particle Size Distribution of N-Sand, M-Sand, and QD.* The particle size distribution for N-sand, M-sand, and QD was carried out in accordance with BS 882-1992 [33]. The particle size distribution for N-sand, M-sand, and QD is shown in Figure 3 and Table 2. According to BS 882-1992 [33], fine aggregates are divided into three grades based on the percentage of passing through standard sieves. It is found that all three types of fine aggregates fall into the category of Grade C sand. The particle size distribution curves for M-sand and QD are overlapped as they have similar particles. Figure 3 shows that N-sand, M-sand, and QD are well graded. Therefore, the composite mix proportions are well graded.

*2.4. Specific Gravity and Absorption of N-Sand, M-Sand, and QD.* Specific gravity and absorption of N-sand, M-sand, and QD were measured (Table 3) according to *ASTM C29/29 M* [34] and *ASTM C128-07a* [35].

*2.5. Mix Design.* The main objective of this research work was to investigate the effect of M-sand and QD on the compressive strength of geopolymer mortar. The binder: fine aggregate, POFA : FA, water/binder, and alkaline activator/binder ratios were kept constant at 1 : 1.5, 1 : 1, 0.2, and 0.4, respectively. Twelve mixtures were produced for the variables of different proportion of N-sand, M-sand, and QD (Table 4).

*2.6. Preparation of Alkaline Activator.* The alkaline activator using sodium hydroxide (NaOH) and sodium silicate ($Na_2SiO_3$) was prepared 24 hours before the casting. Two molarities of sodium hydroxide (NaOH) solution of 12 *M* and 14 *M* were prepared for each mix proportion. The modulus of sodium silicate (i.e., ratio of $SiO_2/Na_2O$) was 2.5 and the specific gravity of liquid $Na_2SiO_3$ was 1.50 g/mL at 20°C. The sodium silicate liquid was mixed with NaOH solution by weight proportion of 1 : 2.5 (NaOH solution : liquid $Na_2SiO_3$).

*2.7. Preparation of Mortar.* The quantities of POFA, FA, alkaline activator, and water used in the mixes were, respectively, 343, 343, 274, and 137 kg/m$^3$. The binder content (POFA : FA) was kept constant at 50 : 50 with the variable of different proportions of fine aggregate contents. The measurements of N-sand, M-sand, and QD used in the mixtures are given in Table 4.

The binder was mixed with the fine aggregates at slow speed (140 ± 5 r/min) in the mixture. The alkaline activator was then added with binder and fine aggregates. The additional water was gradually added to the mixture for good workability.

*2.8. Specimen Preparation and Curing.* The mortar was cast in the 50 mm cube mould and vibrated. The mortar moulds were kept in an oven at 65°C for 24 hours. After removal of the moulds, the specimens were kept in a room temperature and relative humidity of 28°C and 79%, respectively.

*2.9. Flow Table Test.* The flow table test in accordance with ASTM C1437-13 [36] was done to investigate the consistency of mortar.

Table 1: Chemical composition and physical properties of POFA and FA.

(a)

| Chemical compounds | CaO | $SiO_2$ | $Al_2O_3$ | MgO | $Na_2O$ | $SO_3$ | $P_2O_5$ | $K_2O$ | $TiO_2$ | $Cr_2O_3$ | MnO | $Fe_2O_3$ | Cl | LoI |
|---|---|---|---|---|---|---|---|---|---|---|---|---|---|---|
| POFA | 5.57 | 67.72 | 3.71 | 4.04 | 0.16 | 1.07 | 4.13 | 7.67 | 0.27 | — | 0.11 | 4.71 | 0.65 | 6.20 |
| FA | 5.31 | 54.72 | 27.2 | 1.10 | 0.43 | 1.01 | 1.12 | 1.00 | 1.82 | 0.04 | 0.10 | 5.15 | 0.01 | 6.80 |

(b)

| Physical properties | Colour | S.G. | S.S.A. | $D$ [4, 3] | $D$ [3, 2] | $D$ ($v$, 0.1) | $D$ ($v$, 0.5) | $D$ ($v$, 0.9) |
|---|---|---|---|---|---|---|---|---|
| POFA | Black | 2.2 | 3.41 | 20.06 | 3.49 | 3.23 | 18.46 | 38.27 |
| FA | Grey | 2.4 | 1.72 | 36.43 | 1.76 | 0.48 | 16.50 | 101.74 |

S.G.: Specific gravity
S.S.A.: Specific surface area, $m^2/g$
$D$ [4, 3] = Volume moment mean, $\mu$m
$D$ [3, 2] = Surface area moment mean, $(\mu m)^2$
$D$ ($v$, 0.1) = 10% of particle by volume below this size
$D$ ($v$, 0.5) = 50% of particle by volume below this size
$D$ ($v$, 0.9) = 90% of particle by volume below this size.

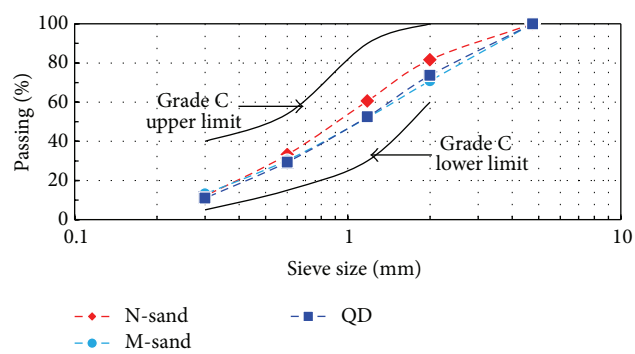


Grade C based on BS EN 933-8-2012
Fineness modulus: 2.88, 2.66 and 2.67 for N-sand, M-sand, QD, respectively

Figure 3: Particle size distribution curve for N-sand, M-sand, and QD.

Table 2: Particle size distribution of N-sand, M-sand, and QD.

| Sieve size | Percentage of passing | | |
|---|---|---|---|
| | N-sand | M-sand | QD |
| 5 mm | 99.99 | 100.00 | 99.98 |
| 2.36 mm | 81.63 | 70.91 | 73.66 |
| 1.18 mm | 60.60 | 52.09 | 52.52 |
| 600 $\mu$m | 33.18 | 30.34 | 29.41 |
| 300 $\mu$m | 12.16 | 13.12 | 11.01 |
| Fineness modulus | 2.88 | 2.66 | 2.67 |
| $D_{10}$, mm | 0.27 | 0.30 | 0.31 |
| $D_{30}$, mm | 0.50 | 0.55 | 1.41 |
| $D_{60}$, mm | 1.24 | 1.42 | 0.57 |
| $C_u = D_{60}/D_{10}$ | 4.53 | 4.80 | 4.56 |
| $C_c = D_{30}{}^2/(D_{10} \times D_{60})$ | 0.74 | 0.73 | 0.74 |

$C_u$: uniformity coefficient; $C_c$: coefficient of curvature.

Table 3: Specific gravity and absorption of N-sand, M-sand, and QD.

| | N-sand | M-sand | QD |
|---|---|---|---|
| | Specific gravity | | |
| SSD | 2.79 | 2.63 | 2.61 |
| Absorption (%) | 0.81 | 0.91 | 0.92 |

OD: Oven Dry.
SSD: saturated surface dry.

Table 4: Mortar mix design.

| Mortar designation | Mix proportions by weight ($kg/m^3$) Fine aggregate | | |
|---|---|---|---|
| | N-Sand | M-Sand | QD |
| M1 | 1029 (100*) | | |
| M2 | 771 (75) | 257 (25) | |
| M3 | 257 (25) | 771 (75) | |
| M4 | | 1029 (100) | |
| M5 | | 257 (75) | 771 (25) |
| M6 | | 771 (25) | 257 (75) |
| M7 | | | 1029 (100) |
| M8 | 257 (25) | | 771 (75) |
| M9 | 771 (75) | | 257 (25) |
| M10 | 514 (50) | 257 (25) | 257 (25) |
| M11 | 257 (25) | 514 (50) | 257 (25) |
| M12 | 257 (25) | 257 (25) | 514 (50) |

* Proportion in percent in bracket ( ).

*2.10. Compressive Strength Test.* The specimens were prepared for 3-, 7-, and 14-day compressive strength tests. The average of three specimens was reported as the compressive strength. The standard deviation was calculated to ascertain any significant change in the test result. The compressive

Table 5: Development of compressive strength for different mix designs.

| Designation | Compressive strength (N/mm$^2$) | | | | | | | |
|---|---|---|---|---|---|---|---|---|
| | Three days | SD | Seven days | SD | 14 days | SD | 28 days | SD |
| **M 1** | **20.75** | **0.63** | **23.34** | **0.34** | **26.83** | **0.23** | **27.80** | **0.40** |
| M 2 | 20.04 | 0.28 | 22.03 | 0.97 | 24.02 | 0.35 | 25.10 | 0.50 |
| M 3 | 18.14 | 0.22 | 19.91 | 0.20 | 24.67 | 0.13 | 25.70 | 0.20 |
| **M 4** | **19.14** | **1.07** | **21.01** | **0.20** | **24.19** | **0.51** | **25.20** | **0.60** |
| M 5 | 17.59 | 1.10 | 19.56 | 0.54 | 22.33 | 0.86 | 23.40 | 0.80 |
| M 6 | 14.75 | 1.18 | 17.76 | 0.63 | 19.36 | 0.25 | 20.50 | 0.70 |
| **M 7** | **21.56** | **0.14** | **23.02** | **0.39** | **25.03** | **0.23** | **26.10** | **0.25** |
| M 8 | 21.45 | 1.00 | 22.90 | 1.21 | 24.90 | 0.97 | 26.00 | 1.06 |
| M 9 | 20.81 | 0.31 | 22.50 | 0.31 | 25.00 | 1.12 | 26.10 | 0.58 |
| M 10 | 17.22 | 0.26 | 20.08 | 0.26 | 22.94 | 0.77 | 24.00 | 0.43 |
| M 11 | 21.28 | 0.64 | 23.10 | 0.70 | 24.92 | 0.75 | 26.00 | 0.60 |
| M 12 | 14.46 | 0.69 | 16.88 | 0.72 | 20.72 | 0.71 | 21.80 | 0.70 |

strength test was carried on according to ASTM C 109/C 109M-12 [37].

## 3. Results and Discussion

*3.1. Density.* The fresh and hardened densities of mortar for different mix proportions at the ages of 3, 7, 14 and 28 days are shown in Figure 4. The fresh densities of the 12 mixes are shown along the X-axis for zero compressive strengths. The fresh and hardened densities vary in the range of 2060–2154 kg/m$^3$ and 1981–2069 kg/m$^3$, respectively. The apparent density increases with the ratio of Si : Al [11]. Since the main variables for different mix proportions in geopolymer mortar are N-sand, M-sand, QD, the specific gravity of these materials influence the variation of densities. Thus the influence of fresh densities of mixes M1 (100% N-sand), M4 (100% M-sand), and M7 (100% QD) of 2146, 2060, and 2060 kg/m$^3$, respectively, could be related to the respective specific gravities of fine aggregates of 2.79 (N-sand), 2.63 (M-sand), and 2.61 (QD).

The changes in density at different ages are influenced by the geopolymerization and curing condition as these undergo several dehydroxylation and crystallization phases at a certain phase [11]. Three types of water release take place during heating from geopolymer concrete, namely, physically bonded water, chemically bonded water, and hydroxyl group ($OH^-$) [11]. The rate of reduction of water from the hardened geopolymer causes the density reduction and it can be seen that this reduction varies from 3.41 to 7.19%. The correlation between the density and compressive strength at different ages of geopolymer mortar is shown in Figure 5. The gradient of compressive strength/density varies between 0.12 and 0.34.

Figure 6 represents the relationship between the density and compressive strength at 28-day age for all mortar specimens. This relationship is comparable with the OPC based mortar/concrete [16]. The densities of the mixes M1 (100% N-sand), M4 (100% M-sand), and M7 (100% QD) at the age of 28-day were found as 2028, 1985, and 1982 kg/m$^3$, respectively (Figure 4). Their respective compressive strengths calculated

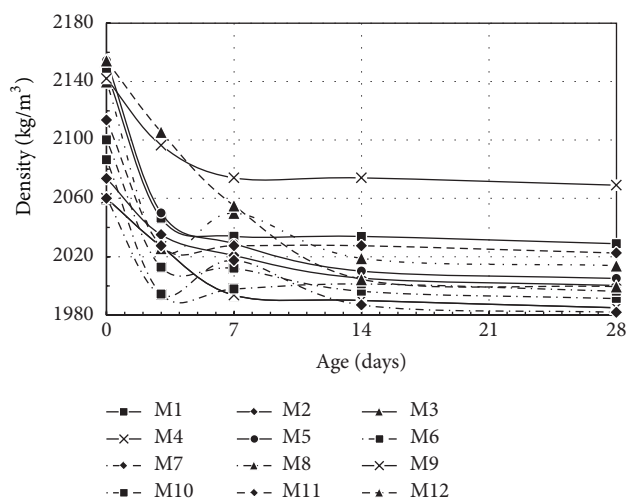


Figure 4: Density versus age (days).

from the equation as given below (Figure 6) were found as 24.32 MPa, 22.97 MPa, and 22.86 MPa, respectively, and these values were close to the experimental results. Consider

$$f'c = 0.0315\rho - 39.558, \quad (1)$$

where $f'c$ and $\rho$ represent compressive strength (MPa) and density (kg/m$^3$).

*3.2. Workability.* The workability results of the mortar found out through flow table test for different mortar mix proportions are shown in Figure 7. The ratios of water:binder and the alkaline solution/binder for all the mix proportions were kept constant. The results show that the flow varied between 43 and 89% and the variation of the consistency (flow, %) might be attributed to the particle texture [8]. The addition of M-sand with N-sand (M2 and M3) slightly reduced the flow. The highest flow of 89% was found for the mix M1 that contained 100% N-sand and this could be attributed to the rounded surface of the N-sand particles [8]. The variation

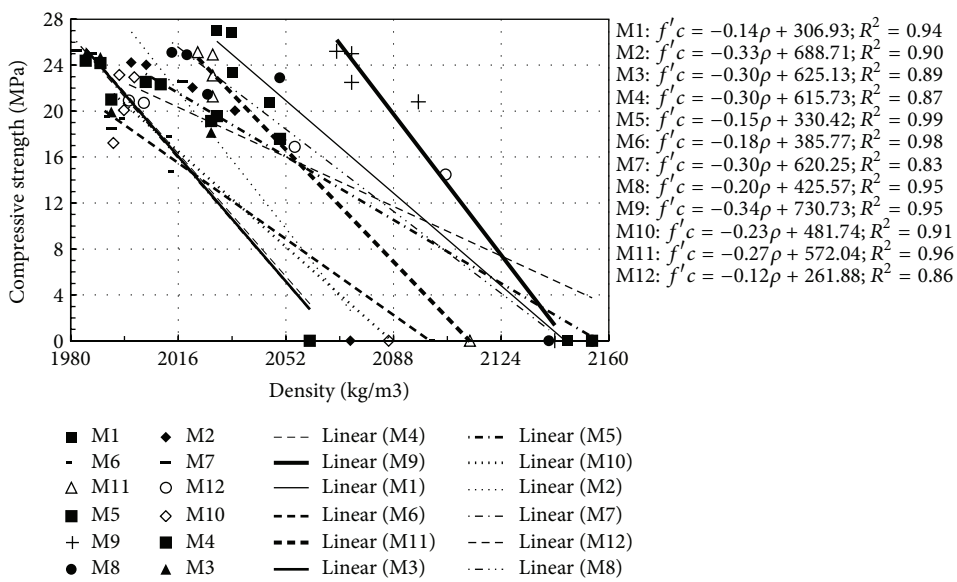


Figure 5: Relationship between density and compressive strength at different ages of mortar mixes.

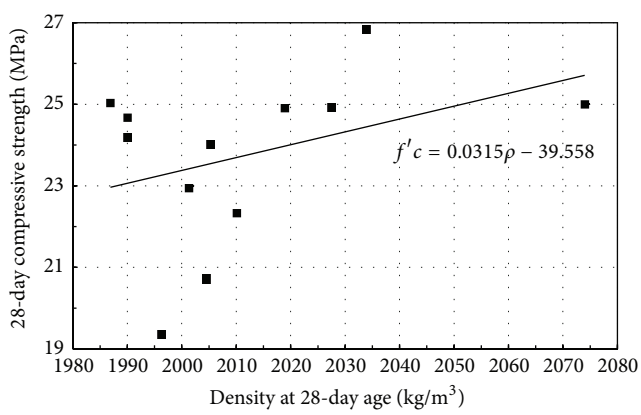


Figure 6: Relationship between density and compressive strength at 28-day age.

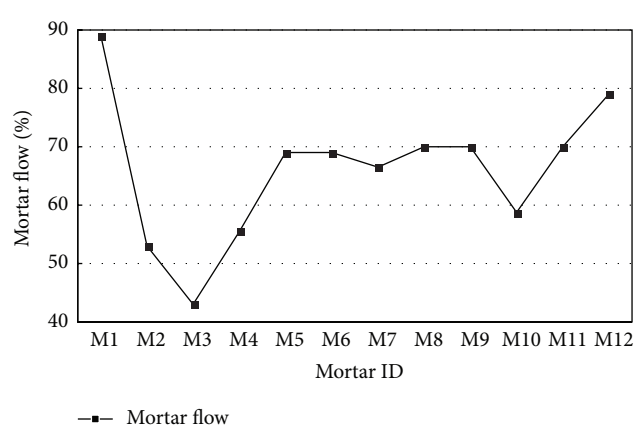


Figure 7: Mortar flow for different mix proportions.

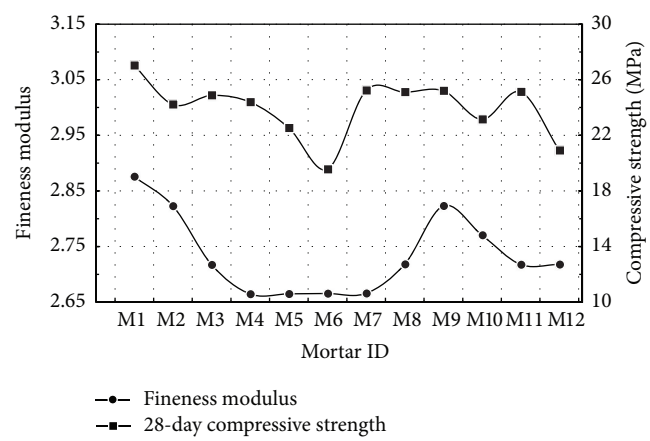


Figure 8: 28-day compressive strength for different mortar mix proportion and the effect of fineness modulus.

of flow is insignificant for the mixes with M-sand and QD (M5 and M6). The flow of M4 shows less flow (55%) than M7 (66%) and one possible explanation could be the better packing ability of M-sand that might have reduced the flow.

*3.3. Development of Compressive Strength.* The compressive strengths for different mix proportions at the ages of 3, 7, 14, and 28 days are shown in Table 5. The 28-day compressive strength for the mixes varied between 21 and 28 N/mm$^2$. The standard deviations as shown in Table 5 were measured from the results found for 3 specimens. The bold values refer to the compressive strength of mortar with 100% N-sand, M-sand, and QD. The average 3-day compressive strength of all mixes was found to be 76% of the 28-day strength.

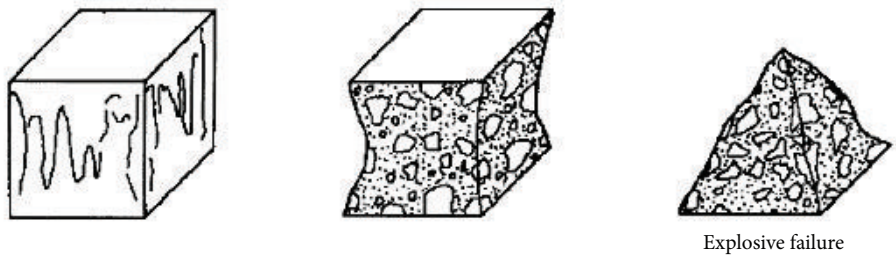


Figure 9: Satisfactory failures (BS EN 12390-3 : 2002).

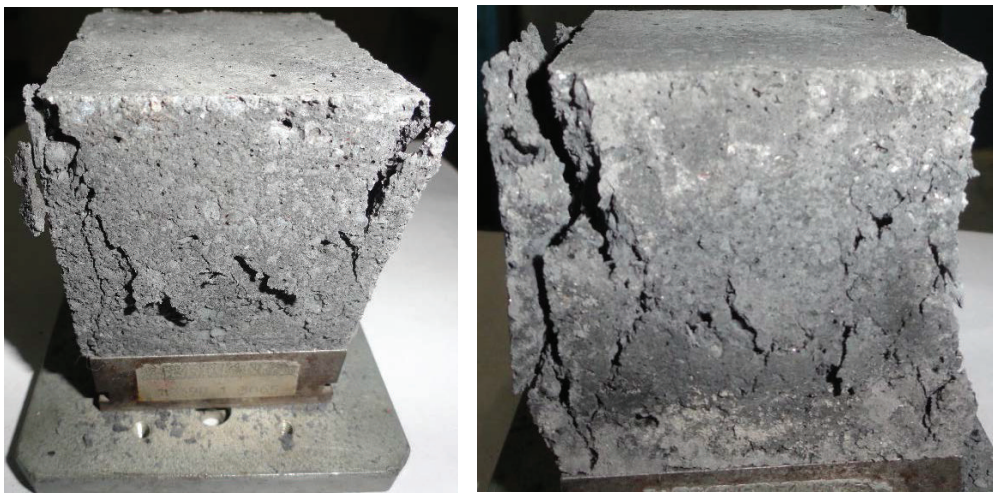

Figure 10: Failure mode.

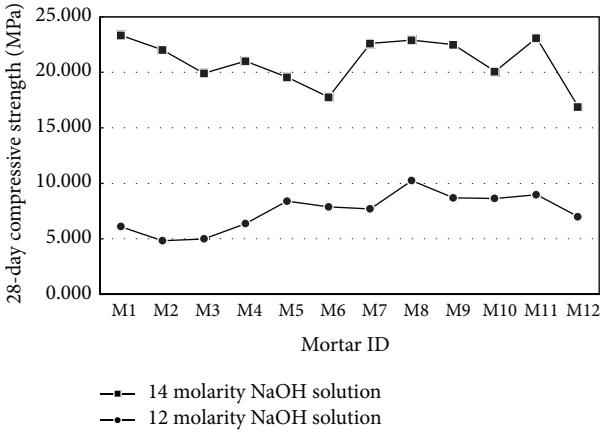


Figure 11: Effect of molarity of alkaline activated solution in compressive strength.

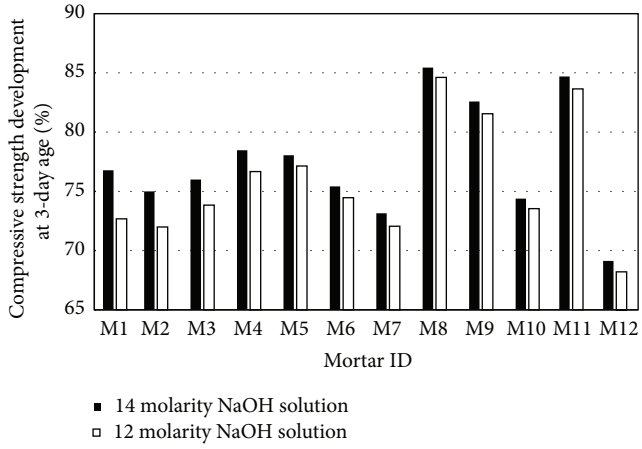


Figure 12: Development of early age compressive strength.

The pattern of early age strength development supports the findings reported by previous researchers [11, 38].

Figure 8 shows the comparison of the compressive strengths for different mortar mixtures with varying proportion of N-sand, M-sand, and QD. Though the mortar with 100% N-sand produced the highest 28-day strength, the combination of N-sand with M-sand and QD reduced the strength. The shape, texture, and particle size distribution affect the compressive strength [8] that might have been attributed to the variation of the compressive strength as seen in Figure 8. The packing density is another factor that influences the workability as well as the compressive strength. Fung et al. [39] cited from Powers [40] that, for a constant volume of binder paste, higher packing density leads to higher workability.

Table 6: Percentage of increment of compressive strength.

| Equations | | Mortar ID | | | | | | | | | | | |
|---|---|---|---|---|---|---|---|---|---|---|---|---|---|
| | | M1 | M2 | M3 | M4 | M5 | M6 | M7 | M8 | M9 | M10 | M11 | M12 |
| Three to 7 day | $\frac{S7 - S3}{S3} \times 100$ | 12.5 | 9.9 | 9.8 | 9.8 | 11.2 | 20.4 | 6.8 | 6.8 | 8.1 | 16.6 | 8.6 | 16.8 |
| Seven to 14 day | $\frac{S14 - S7}{S7} \times 100$ | 14.9 | 9.0 | 23.9 | 15.1 | 14.2 | 9.0 | 8.8 | 8.8 | 11.1 | 14.3 | 7.9 | 22.7 |
| 14 to 28 day | $\frac{S28 - S14}{S3} \times 100$ | 3.7 | 4.2 | 4.1 | 4.1 | 4.5 | 5.2 | 4.0 | 4.0 | 4.0 | 4.4 | 4.0 | 4.8 |

$S3$, $S7$, $S14$, and $S28$ are the compressive strengths at 3, 7, 14, and 28 days, respectively.

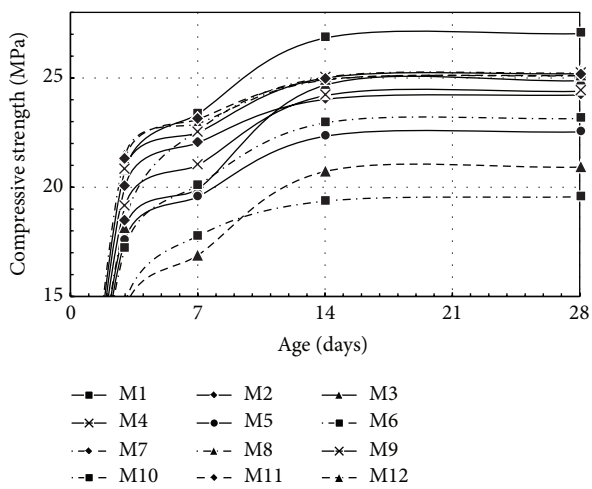


Figure 13: Compressive strength (MPa) versus age (days).

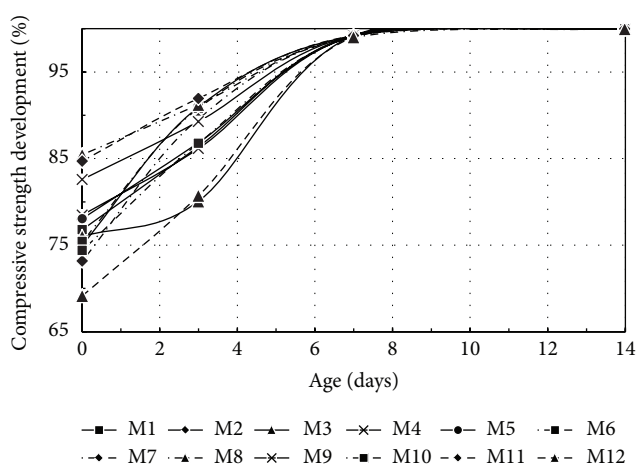


Figure 14: % of compressive strength development versus age (days).

*3.4. Failure Mode.* The failure mode of N-sand/M-sand/QD based geopolymer mortar was found to be similar to the N-sand based cement mortar. Also, the mode of failure was found satisfactory as specified in BS EN 12390-3:2002 (Figures 9 and 10).

*3.5. Role of POFA-FA on the Development of Compressive Strength.* The high content of pozzolanic silica and alumina in POFA and FA causes the silica based geopolymerization in presence of alkaline solution. The silica/alumina ratio and total content of silica, alumina, and $Fe_2O_3$ affect the strength development [11]. It is to be noted that the binders, POFA, and FA were kept at equal proportions for all the mixes. The silica/alumina ratio and the total contents of silica, alumina, and $Fe_2O_3$ in the POFA-FA mixture were found to be 3.95 and 82%, respectively, and Autef et al. [41] reported that high amount of silica content increased the rate of geopolymerization.

As seen from Table 1, 90% of particles of POFA and FA were found below 38.27 and 101.74 $\mu$m, respectively. The finer particles decrease the capillary pore effectively [42]. The angular and irregular shaped QD particles create voids within the mortar. The filler effect of the fine FA and POFA might reduce the voids and Ashtiani et al. [43] reported that higher packing factor enhanced the compressive strength.

The effect of oven curing on the strength development also plays significant role in geopolymer mortar as seen from the 3-day compressive strength; as seen from Table 6, the achievement of 76% of 28-day compressive strength at the age of 3-day is attributed to the heat curing in oven at 65°C temperature for 24 hours. However, the rate of strength increment from 3 days to 7 days was found between 12 and 16% and beyond 7 days, it is much lower as reported by Alexander and Mindess [44]. Similar finding on high early strength development due to heat curing at elevated temperature was reported elsewhere [11, 45]. The fineness of POFA and FA also has significant effect on the development of early age strength at 3 days. The finer particles have larger surface area that may increase the reactivity in the geopolymerization process [46].

*3.6. Effect of Particle Size of N-Sand/M-Sand/QD on Geopolymerization.* Tasong et al. [47] reported that a wide range of chemical interactions are anticipated within the interfacial transition zone between aggregate and cement paste matrix. Isabella et al. [48] found a positive effect on the addition of soluble silicates into leaching solution by promoting significant structural breakdown of sand and metakaolin; they also reported that larger surface area of the aggregate interacted with soluble silicates releasing a greater amount of Si. It is conceivable that the fine particles of N-sand/M-sand/QD may interact with the alkaline solution in mortar; the rate of interaction with N-sand, M-sand, and QD surfaces may be related to their particle surface area. A strong bonding between geopolymer matrix and the aggregate surface by the

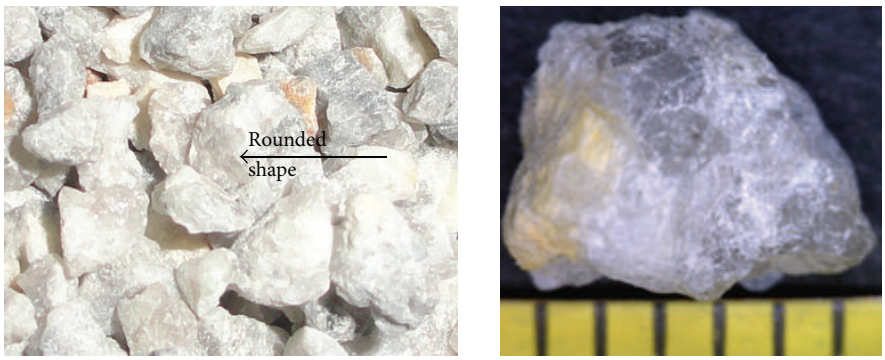


Figure 15: Shape of manufactured sand particle (2.36 mm retained).

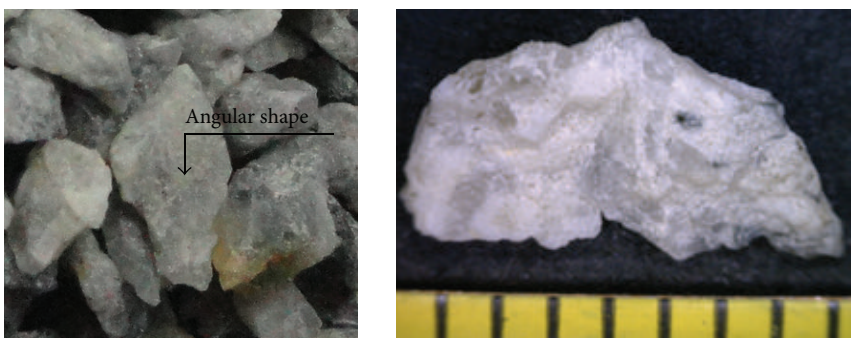


Figure 16: Shape of quarry dust particle (2.36 mm retained).

ionic interaction may exist [49] and this could enhance the development of compressive strength of N-sand/M-sand/QD based geopolymer mortar.

*3.7. Effect of Molarity of Alkaline Activated Solution on Development of Compressive Strength.* The effect of molarity of alkaline activated solution (NaOH solution) on the 28-day compressive strength is shown in Figure 11. As shown in Figure 12, development of early age compressive strength, the early age compressive strength at the age of 3 days for the mix with 14 *M* was found between 55 and 77% of the 28-day strength and this is higher than the corresponding strength of mixes with 12 *M*. The use of low concentrated alkaline solution causes a weak reaction [50]. The compressive strength increase in the mixes with high molarity based alkaline solution was due to the leaching of silica and alumina [51]. The NaOH concentration performs the dissolution process and bonding of solid particles in the geopolymeric environment [52]. The use of high concentration of NaOH solution leads to greater dissolution and increases the geopolymerization reaction [53] and this is supported by various studies [46, 54–56].

*3.8. Effect of Fineness Modulus on Compressive Strength.* Figure 8 shows the variation of fineness modulus due to the different mix proportion of N-sand, M-sand, and QD. The fineness modulus for the composite mix proportion was calculated by arithmetic proportion [44]. For example, mortar ID M11 represents N-sand : M-sand : QD = 25 : 50 : 25:

$$\begin{aligned}&\text{Fineness modulus (FM) for M11}\\&= \mathrm{FM}_{\text{N-sand}} \times 0.25 + \mathrm{FM}_{\text{M-sand}}\\&\times 0.50 + \mathrm{FM}_{\text{QD}} \times 0.25 = 2.72.\end{aligned} \tag{2}$$

Hence, the fineness moduli of the various combination of the fine aggregates using N-sand, M-sand, and QD vary from 2.66 to 2.88 The values of fineness modulus of the combined fine aggregates in this investigation fall in the medium range based on the classification as proposed by Alexander and Mindess [44]. It is to be noted that the binder content is kept constant for all the mixes. The mixes with more fine particles need large volume of paste as the surface area is more. The variation in the compressive strength of the mortars between 20.36 and 26.03 MPa could be attributed to the paste volume and the fineness or coarseness of the fine aggregates.

*3.9. Effect of N-Sand, M-Sand, and QD on Development of Compressive Strength.* The compressive strengths at different ages along with their respective percentages with age are shown in Figures 13 and 14. The mortar using 100% N-sand shows better compressive strength performance than the mix with M-sand. The replacement of N-sand by M-sand reduces compressive strength.

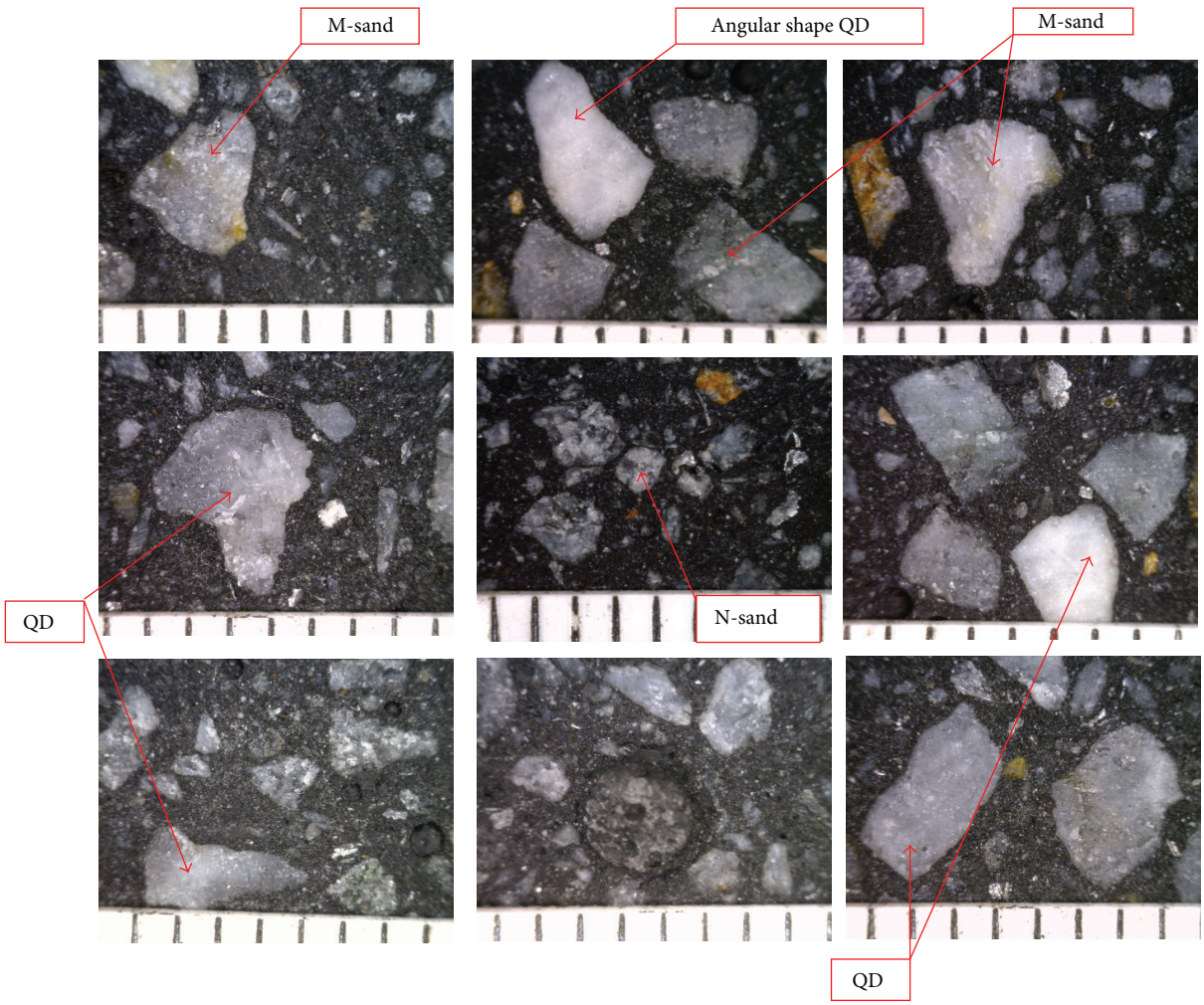


Figure 17: N-sand/M-sand/QD interlocking in geopolymer mortar.

The N-sand contains rounder and smoother particle than M-sand (Figure 15) [8] and QD (Figure 16). Hudson [57] reported that rough aggregates have a propensity for increasing water demand for a given workability. Thus, for a given water content, the N-sand is more workable than M-sand [8]. The rough surfaces of M-sand particles demand more water than N-sand. In this study, the water and binder content was kept constant. This could lead to absorption of water from the alkali solution and this might have affected the reactivity of binder in alkali solution. Thus, the reduction of the compressive strength due to the replacement of N-sand by M-sand could be attributed to absorption of water by the rough surfaces of M-sand.

The 28-day compressive strengths of about 28 MPa and 25 MPa were obtained for specimens with 100% N-sand and 100% M-sand, respectively. The reduction of strength between these two mixes was found to be only 3 MPa and similar finding on the strength difference for M-sand and N-sand was reported by Dumitru et al. [58].

The mortar using 100% QD shows better performance than the mix with M-sand in Figures 13 and 14. The presence of high percentage of QD in composite fine aggregate mixture of M-sand and QD reduces the strength (M5, M6). The particle shape and texture may influence the strength reduction.

The QD has sharp angular particles as shown in Figure 16. According to Quiroga and Fowler [8] and Kaplan [59], the angularity of aggregates has a positive effect on the compressive strength. Further, the angularity of the aggregates enhances the bond between the matrix and the aggregates due to its surface texture. Galloway [60] also reported the effect of surface texture on the strength significantly as rough surface increases bonding between the aggregate surface and the paste.

Figure 17 shows the interlocking of N-sand/M-sand/QD in geopolymer mortar. The combination of M-sand and QD might tend to create voids due to the combination of semirounded particles and the sharp angular particles. Further, the increase in voids demands more water for a given workability and hence decreases the strength [8]. Since the water : binder ratio was maintained constant for all the mixes, the composite mixes that contained both M-sand and QD might have absorbed more water that could influence the geopolymerization process. This might reduce the strength for mixes with high percentage of QD in the

Table 7: Development of compressive strength using N-sand, M-sand, and QD.

| Age | 3-day | | 7-day | | 14-day | | 28-day | |
|---|---|---|---|---|---|---|---|---|
| Fine aggregate | NC | GM | NC | GM | NC | GM | NC | GM |
| N-sand (100%) | 22 | 21 | 28 | 23 | 33 | 27 | 37 | 28 |
| M-Sand (100%) | 15 | 19 | 23 | 21 | 26 | 24 | 32 | 25 |
| QD (100%) | 19 | 21 | 28 | 23 | 32 | 25 | 37 | 26 |

NC: results from [Dumitru et al. [58]] experiment on OPC concrete.
GM: results from this experiment on geopolymer mortar.

mixes that contained both the M-sand and QD. Nevertheless, the strength reduction between the mixes with 100% QD and 100% M-sand was negligible and similar finding was reported by Dumitru et al. [58].

Figures 13 and 14 show that there is not much significant difference in the compressive strength due to the replacement of N-sand by QD either partially or fully. The mixes with N-sand developed better strength due to its well-graded and round particles. As mentioned the angularity of QD particles enhances the compressive strength, and for a given workability, the rough surface increases water demand [8].

The 28-day compressive strength of mixes with N-sand and QD were 28 MPa and 26 MPa, respectively. Again, the strength difference between these two mixes was about 2 MPa and negligible. Raman et al. [61] found the similar effect of QD in rice husk ash based concrete and reported that inclusion of QD as partial replacement for sand slightly decreases the compressive strength of concrete. Dumitru et al. [58] reported that the replacement of N-sand by QD produces comparable strength and hence QD is viable replacement to conventional N-sand for sustainable material.

*3.10. Comparison of M-Sand and QD in Geopolymer Mortar with Published Data.* Dumitru et al. [58] investigated the effect of river sand, manufactured quarry fines, and unprocessed quarry fines that are comparable to the research materials N-sand, M-sand, and QD, respectively, used in this research work.

The development of 3-, 7-, 14- and 28-day compressive strength is quite similar to the outcome from this investigation, as seen from Table 7. The effect of QD, M-sand, and N-sand in both normal concrete (NC) and geopolymer mortar (GM) between the 3 and 14 days shows similar trends, albeit these are different kinds of concretes. As known, the geopolymer concrete develops high early strength due to geopolymerization and hence the strength difference between the 14- and 28-day strength was not much different, unlike normal concrete where the strength development continues beyond 14 days.

## 4. Conclusions

(1) The mix with 100% replacement of N-sand by QD showed higher compressive strength compared to replacing N-sand by different proportion of M-sand and QD.

(2) Though the compressive strength slightly reduces due to the replacement of N-sand or QD by M-sand, the M-sand is considered as a viable alternative to conventional sand due to depletion of natural resources. The slight variation in the compressive strength might be attributed to the aggregate shape and texture.

(3) The usage of 100% M-Sand in POFA-FA-based geopolymer mortar produced comparable strength as that of 100% N-sand.

(4) The use of QD as fine aggregate also reinforces the use of waste material as replacement for conventional N-sand; the high strength of specimens with 100% QD is attributed to the rough surfaces of QD that enhances the bond between the paste and the aggregates.

(5) The replacement of conventional N-sand with M-sand and QD shows comparable strength as that of N-sand based specimens and the use of M-sand and QD is recommended in geopolymer concrete.

(6) The high concentration of sodium hydroxide solution increases the compressive strength.

(7) The mixes with more fine particles require more paste to cover the surface areas, but for the mixes with constant binder content, the influence of the finer particles cannot be ignored.

(8) The failure mode of geopolymer mortar was found similar to that of Portland cement mortar.

(9) The density and compressive strength relationship of N-sand/M-sand/QD based geopolymer mortar was also found similar to that of the Portland cement mortar.

## Conflict of Interests

The authors declare that there is no conflict of interests regarding the publication of this paper.

## Acknowledgment

The authors are grateful to University of Malaya for the financial support through the University of Malaya Research Project *"RP018/2012B: Development of Geopolymer Concrete for Structural Application."* The research focuses on the development of geopolymer composite mortar using sustainable materials such as fly ash (FA) and palm oil fuel ash (POFA) as

binders. The research material can be accessed through SAGE publication and through University of Malaya library.

## References


[1] U. J. Alengaram, B. A. A. Muhit, and M. Z. B. Jumaat, "Utilization of oil palm kernel shell as lightweight aggregate in concrete—a review," *Construction and Building Materials*, vol. 38, pp. 161–172, 2013.

[2] S. Rukzon and P. Chindaprasirt, "Use of disposed waste ash from landfills to replace Portland cement," *Waste Management & Research*, vol. 27, no. 6, pp. 588–594, 2009.

[3] M. Safiuddin, U. J. Alengaram, M. A. Salam, M. Z. Jumaat, F. F. Jaafar, and H. B. Saad, "Properties of high-workability concrete with recycled concrete aggregate," *Materials Research*, vol. 14, no. 2, pp. 248–255, 2011.

[4] M. Safiuddin, M. A. Salam, and M. Z. Jumaat, "Utilization of palm oil fuel ash in concrete: a review," *Journal of Civil Engineering and Management*, vol. 17, no. 2, pp. 234–247, 2011.

[5] P. Appukutty and R. Murugesan, "Substitution of quarry dust to sand for mortar in brick masonry works," *International Journal on Design and Manufacturing Technologies*, vol. 3, pp. 59–63, 2009.

[6] M. Westerholm, B. Lagerblad, J. Silfwerbrand, and E. Forssberg, "Influence of fine aggregate characteristics on the rheological properties of mortars," *Cement and Concrete Composites*, vol. 30, no. 4, pp. 274–282, 2008.

[7] J. M. Shilstone, "The aggregate: the most important value-adding component in concrete," in *Proceedings of the 7th Annual Symposium*, International Center for Aggregates Research (ICAR), Austin, Tex, USA, 1999.

[8] P. N. Quiroga and D. W. Fowler, *The Effects of Aggregates Characteristics on the Performance of Portland Cement Concrete*, International Centre for Aggregates Research (ICAR), The University of Texas at Austin, Austin, Tex, USA, 2004.

[9] B. P. Hudson, "Modification to the fine aggregate angularity test," in *Proceedings of the 7th Annual Symposium*, International Center for Aggregates Research (ICAR), Austin, Tex, USA, 1999.

[10] M. L. Marceau, M. A. Nisbet, and M. G. VanGeem, "Life cycle inventory of Portland cement concrete," 5420 Old Orchard Road, Skokie, Illinois 60077-1083: Portland Cement Association, 2007.

[11] J. Davidovits, *Geopolymer Chemistry & Application*, Institute Géopolymèr, Saint-Quentin, France, 3rd edition, 2008.

[12] S. Thokchom, P. Ghosh, and S. Ghosh, "Durability of fly ash geopolymer mortars in nitric ACID—effect of alkali ($Na_2O$) content," *Journal of Civil Engineering and Management*, vol. 17, no. 3, pp. 393–399, 2011.

[13] A. S. M. A. Awal and M. W. Hussin, "The effectiveness of palm oil fuel ash in preventing expansion due to alkali-silica reaction," *Cement and Concrete Composites*, vol. 19, no. 4, pp. 367–372, 1997.

[14] M. W. Hussin and A. S. M. A. Awal, "Influence of palm oil fuel ash on strength and durability of concrete," in *Proceedings of the 7th International Conference on Durability of Building Materials and Components*, pp. 291–298, E & FN Spon, London, UK, 1996.

[15] J. Žvironaitė, I. Pundienė, S. Gaidučis, and V. Kizinievič, "Effect of different pozzolana on hardening process and properties of hydraulic binder based on natural anhydrite," *Journal of Civil Engineering and Management*, vol. 18, pp. 530–536, 2012.

[16] S. Chandra and L. Berntsson, *Light Weight Aggregate Concrete*, Noyels Publications, Norwich, NY, USA, 2002.

[17] P. Shafigh, U. J. Alengaram, H. B. Mahmud, and M. Z. Jumaat, "Engineering properties of oil palm shell lightweight concrete containing fly ash," *Materials & Design*, vol. 49, pp. 613–621, 2013.

[18] S. P. Yap, U. J. Alengaram, and M. Z. Jumaat, "Enhancement of mechanical properties in polypropylene- and nylon-fibre reinforced oil palm shell concrete," *Materials and Design*, vol. 49, pp. 1034–1041, 2013.

[19] U. Johnson Alengaram, B. A. Al Muhit, M. Z. bin Jumaat, and M. L. Y. Jing, "A comparison of the thermal conductivity of oil palm shell foamed concrete with conventional materials," *Materials and Design*, vol. 51, pp. 522–529, 2013.

[20] T. Weng, W. Lin, and A. Cheng, "Effect of metakaolin on strength and efflorescence quantity of cement-based composites," *The Scientific World Journal*, vol. 2013, Article ID 606524, 11 pages, 2013.

[21] M. Safiuddin, M. H. M. Isa, and M. Z. Jumaat, "Fresh properties of self-consolidating concrete incorporating palm oil fuel ash as a supplementary cementing material," *Chiang Mai Journal of Science*, vol. 38, no. 3, pp. 389–404, 2011.

[22] S. K. Lim, C. S. Tan, O. Y. Lim, and Y. L. Lee, "Fresh and hardened properties of lightweight foamed concrete with palm oil fuel ash as filler," *Construction and Building Materials*, vol. 46, pp. 39–47, 2013.

[23] N. M. Altwair, M. A. Megat Johari, and S. F. Saiyid Hashim, "Flexural performance of green engineered cementitious composites containing high volume of palm oil fuel ash," *Construction and Building Materials*, vol. 37, pp. 518–525, 2012.

[24] W. Kroehong, T. Sinsiri, and C. Jaturapitakkul, "Effect of palm oil fuel ash fineness on packing effect and pozzolanic reaction of blended cement paste," *Procedia Engineering*, vol. 14, pp. 361–369, 2011.

[25] M. M. Tamim, A. Dhar, and M. S. Hossain, "Fly ash in Bangladesh–an overview," *International Journal of Scientific & Engineering Research*, vol. 4, pp. 809–812, 2013.

[26] N. K. Lee and H. K. Lee, "Setting and mechanical properties of alkali-activated fly ash/slag concrete manufactured at room temperature," *Construction and Building Materials*, vol. 47, pp. 1201–1209, 2013.

[27] C. Nagiah and R. Azmi, "A review of smallholder oil palm production: challenges and opportunities for enhancing sustainability—a Malaysian perspective," *Journal of Oil Palm & the Environment*, vol. 3, pp. 114–120, 2012.

[28] N. M. Altwair, M. A. M. Johari, and S. F. S. Hashim, "Influence of treated palm oil fuel ash on compressive properties and chloride resistance of engineered cementitious composites," *Materials and Structures*, pp. 1–16, 2013.

[29] A. Hawa, D. Tonnayopas, and W. Prachasaree, "Performance evaluation and microstructure characterization of Metakaolin-based geopolymer containing Oil Palm Ash," *The Scientific World Journal*, vol. 2013, Article ID 857586, 9 pages, 2013.

[30] S. E. Wallah and B. V. Rangan, "Low-calcium fly ash-based geopolymer concrete: long-term properties," Research Report GC 2, Engineering Faculty, Curtin University of Technology, Perth, Australia, 2006.

[31] D. Hardjito, S. E. Wallah, D. M. J. Sumajouw, and B. V. Rangan, "On the development of fly ash-based geopolymer concrete," *Australian Journal of Structural Engineering*, vol. 6, no. 6, Article ID 101-M52, pp. 77–84, 2005.

[32] R. H. Kupaei, U. J. Alengaram, M. Z. B. Jumaat, and H. Nikraz, "Mix design for fly ash based oil palm shell geopolymer lightweight concrete," *Construction and Building Materials*, vol. 43, pp. 490–496, 2013.

[33] British Standard BS 882, *Specification for Aggregates from Natural Sources for Concrete*, British Standards Institute, 1992.

[34] ASTM Standard C29/C29M-09, *Standard Test Method for Bulk Density (Unit Weight) and Voids in Aggregate*, ASTM International, West Conshohocken, Pa, USA, 2009.

[35] ASTM C128-12, *Standard Test Method for Density, Relative Density (Specific Gravity), and Absorption of Fine Aggregate*, ASTM International, West Conshohocken, Pa, USA.

[36] ASTM International, "Standard test method for flow of hydraulic cement mortar," ASTM C1437-13, ASTM International, West Conshohocken, Pa, USA.

[37] ASTM International C 109/C 109M, *Standard Test Method for Compressive Strength of Hydraulic Cement Mortars (Using 2-in or [50-mm] Cube Specimens)*, ASTM International, West Conshohocken, Pa, USA, 1999.

[38] N. Lloyd and V. Rangan, "Geopolymer concrete-sustainable cementless concrete," *ACI Special Publication*, vol. 261, pp. 33–54, 2009.

[39] W. W. S. Fung, A. K. H. Kwan, and H. H. C. Wong, "Wet packing of crushed rock fine aggregate," *Materials and Structures*, vol. 42, no. 5, pp. 631–643, 2009.

[40] T. C. Powers, *The Properties of Fresh Concrete*, Road Research Laboratory, Hoboken, NJ, USA, 1969.

[41] A. Autef, E. Joussein, G. Gasgnier, and S. Rossignol, "Role of the silica source on the geopolymerization rate: a thermal analysis study," *Journal of Non-Crystalline Solids*, vol. 366, no. 1, pp. 13–21, 2013.

[42] P. Chindaprasirt, C. Jaturapitakkul, and T. Sinsiri, "Effect of fly ash fineness on microstructure of blended cement paste," *Construction and Building Materials*, vol. 21, no. 7, pp. 1534–1541, 2007.

[43] M. S. Ashtiani, A. N. Scott, and R. P. Dhakal, "Mechanical and fresh properties of high-strength self-compacting concrete containing class C fly ash," *Construction and Building Materials*, vol. 47, pp. 1217–1224, 2013.

[44] M. Alexander and S. Mindess, *Aggregates in Concrete*, Taylor & Francis, Abingdon, UK, 2005.

[45] S. Pangdaeng, T. Phoo-Ngernkham, V. Sata, and P. Chindaprasirt, "Influence of curing conditions on properties of high calcium fly ash geopolymer containing Portland cement as additive," *Materials & Design*, vol. 53, pp. 269–274, 2014.

[46] K. Somna, C. Jaturapitakkul, P. Kajitvichyanukul, and P. Chindaprasirt, "NaOH-activated ground fly ash geopolymer cured at ambient temperature," *Fuel*, vol. 90, no. 6, pp. 2118–2124, 2011.

[47] W. A. Tasong, J. C. Cripps, and C. J. Lynsdale, "Aggregate-cement chemical interactions," *Cement and Concrete Research*, vol. 28, no. 7, pp. 1037–1048, 1998.

[48] C. Isabella, G. C. Lukey, H. Xu, and J. S. J. V. Deventer, "The effect of aggregate particle size on formation of geopolymeric gel," in *Advanced Materials for Construction of Bridges, Buildings and Other Structures III*, V. Mistry, A. Azizinamini, and J. M. Hooks, Eds., ECI Digital Archives, Davos, Switzerland, 2003.

[49] W. K. W. Lee and J. S. J. van Deventer, "Chemical interactions between siliceous aggregates and low-Ca alkali-activated cements," *Cement and Concrete Research*, vol. 37, no. 6, pp. 844–855, 2007.

[50] F. Puertas, S. Martínez-Ramírez, S. Alonso, and T. Vázquez, "Alkali-activated fly ash/slag cements. Strength behaviour and hydration products," *Cement and Concrete Research*, vol. 30, no. 10, pp. 1625–1632, 2000.

[51] P. Chindaprasirt, C. Jaturapitakkul, W. Chalee, and U. Rattanasak, "Comparative study on the characteristics of fly ash and bottom ash geopolymers," *Waste Management*, vol. 29, no. 2, pp. 539–543, 2009.

[52] E. Álvarez-Ayuso, X. Querol, F. Plana et al., "Environmental, physical and structural characterisation of geopolymer matrixes synthesised from coal (co-)combustion fly ashes," *Journal of Hazardous Materials*, vol. 154, no. 1–3, pp. 175–183, 2008.

[53] X. Guo, H. Shi, and W. A. Dick, "Compressive strength and microstructural characteristics of class C fly ash geopolymer," *Cement and Concrete Composites*, vol. 32, no. 2, pp. 142–147, 2010.

[54] G. Kovalchuk, A. Fernández-Jiménez, and A. Palomo, "Alkali-activated fly ash: effect of thermal curing conditions on mechanical and microstructural development—part II," *Fuel*, vol. 86, no. 3, pp. 315–322, 2007.

[55] D. Hardjito, C. C. Cheak, and C. H. L. Ing, "Strength and setting times of low calcium fly ash-based geopolymer mortar," *Modern Applied Science*, vol. 2, pp. 3–11, 2009.

[56] F. A. Memon, M. F. Nuruddin, S. Khan, N. Shafiq, and T. Ayub, "Effect of sodium hydroxide concentration on fresh properties and compressive strength of self-compacting geopolymer concrete," *Journal of Engineering Science and Technology*, vol. 8, no. 1, pp. 44–56, 2013.

[57] B. P. Hudson, "Concrete workability with high fines content sands," *Quarry*, vol. 7, pp. 22–25, 1999.

[58] I. Dumitru, T. Zdrilic, and G. Smorchevsky, "The use of manufactured quarry fines in concrete," in *Proceedings of the 7th Annual Symposium on Aggregates-Concrete, Bases and Fines*, pp. C1-5-1–C1-5-12, International Centre for Aggregates Research (ICAR), Austin, Tex, USA, 1999.

[59] M. Kaplan, *The Fle xural and Compressive Strength of Concrete as Affected by the Properties of Coarse Aggregates*, National Building Research Institute, Council for Scientific and Industrial Research (CSIR), 1960.

[60] J.E. Galloway, "Grading, Shape and Surface Properties," ASTM International, 1994.

[61] S. N. Raman, T. Ngo, P. Mendis, and H. B. Mahmud, "High-strength rice husk ash concrete incorporating quarry dust as a partial substitute for sand," *Construction and Building Materials*, vol. 25, no. 7, pp. 3123–3130, 2011.

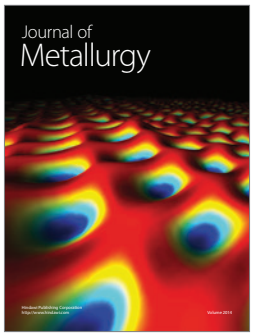

Hindawi

Submit your manuscripts at
http://www.hindawi.com